

A Decentralized Multi-Robot Object Transportation Exploiting Surrounding Obstacles

Gyuhoo Eoh

Chungbuk National University, Cheongju, South Korea

Email: gyuhoo.eoh@gmail.com

Abstract—This paper presents a cooperative object transportation technique exploiting surrounding obstacles. In previous studies, obstacles have been considered only an impediment during the transportation process. Robots should explore a detour route when they encounter obstacles. In some cases, however, obstacles are not merely obstructions, but they can help generate a transport path to a goal. In this paper, robots generate an enclosing object transportation formation using surrounding obstacles. The surrounding obstacles replace the particular role of robots, especially path guidance function. The enclosing formation consists of robots and obstacles and continuously changes its shape to transport objects to a goal. In addition, each robot can decide its own action with a limited sensing range, and robots can transport multiple objects through narrow paths between obstacles. Simulation and practical experiments are presented to verify the proposed method.

Index Terms—decentralized control, multi-robot, object transportation, robot formation, virtual electric dipole field

I. INTRODUCTION

An object transportation using multiple robots has been considered to be an important subject in diverse fields such as logistics [1], exploration [2], rescue [3], and foraging [4]. A large or heavy object can be easily transported using multi-robot cooperation inspired by collective nature's behaviors such as ants [5] or bees [6], because the behaviors of multiple robots are more efficient and flexible than those of a single robot. Therefore, many researchers have investigated how to transport objects efficiently [7], and there are three major object transportation methods: *grasping*, *pushing*, and *caging*.

First, multiple robots grasp an object with manipulators and transport it to a desired goal [8]–[10]. This grasping method shows stable movement, because the object is connected to robots with manipulators. Robots do not have to consider the movement of an object during the transportation process, which facilitates object transportation without a complex controller. However, robots need preliminary grasping and synchronized actions for object transportation. Second, multiple robots transport an object using pushing behavior [11]–[13]. Preliminary grasping action is unnecessary in the pushing technique, which enables robots to manipulate a large object by relatively simple action. But robots should watch the movement of objects during object transportation because objects sometimes show unexpected motions when robots

push them. Thus, some researchers have presented a pusher-watcher framework to coordinate a robot team [14]. Finally, there is a caging technique in which a multi-robot team transports multiple objects by enclosing them [15]–[17]. The objects cannot escape from an enclosing robot formation, which enables multiple objects to be manipulated easily. However, robot formation can be easily broken during transportation, and an excessive number of robots is required for object transportation.

To solve these issues, our previously proposed studies have suggested a new cooperative object transportation based on cyclic motion [18], [19]. Multiple robots formulate two parallel line formations and push multiple objects into the formation with cyclic motion. It is possible to transport objects without escaping from the robot formation because only a part of robots moves during object transportation. In this object transportation technique, there is an assumption that obstacles do not exist. However, there are multiple obstacles in the real environment, and thus, we should consider these obstacles for practical object transportation techniques. If our previously proposed techniques are applied in a static environment where obstacles exist, the guider robot will collide with the obstacles or a large region needs for object transportation, as shown in Fig.1(a) and Fig.1(b), respectively.

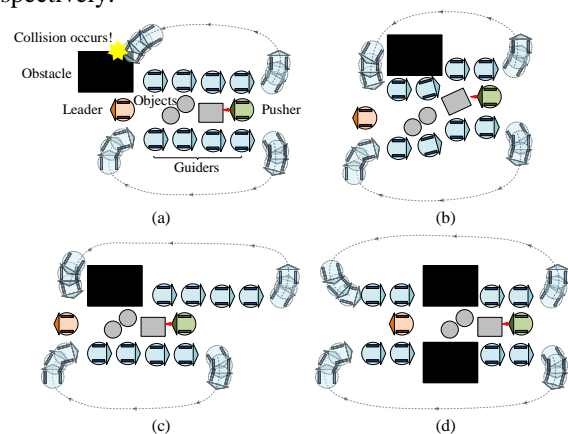


Figure 1. (a) Collision can occur in a static environment when guider robots approach the head robot because the obstacles prevent the movement of the guider robot. (b) It needs excessive space to transport objects and guider robots are difficult to locate in the desired position. (c) An obstacle can help object transportation by preventing the escape of objects. (d) Objects can be transported in a narrow way using the proposed method.

We, therefore, present a novel cooperative multi-object transportation technique in which surrounding obstacles replace the part of guider robots. If the guider robot is located next to an obstacle, the obstacle can be used as a path-guided block to prevent the object from escaping, as shown in Fig.1(c). This method has two advantages by comparison with previous techniques. First, object transportation is possible only using fewer robots because obstacles replace the role of guider robots which prevent objects from escaping. Second, the objects can be transported through a narrow path using surrounding obstacles, as shown in Fig.1(d).

This paper is organized as follows. Section II presents the problem statement and section III describes the preliminaries of this paper. Section IV explains cooperative object transportation in a static environment, and section V shows finite state machines of the proposed technique. Sections VI and VII show simulation and practical experiments, respectively. Finally, section VIII presents a conclusion.

II. PROBLEM STATEMENT

A. Assumptions

To address the object transportation problem, the following assumptions are made. First, all robots are modelled in identical-sized circles, which move in a two-dimensional plane. Additionally, all robots have two differential wheeled driving characteristics. Second, we assume that the roles of each robot are predefined as the *guider*, *pusher*, or *leader* before transportation. The guider robots cannot be pushed by objects or other robots; they take the role of path guidance. The pusher robot has sufficient power to push multiple objects. The leader robot generates a global path and leads the multi-robot team to a goal. Various path planners can be used for global path planning, such as visibility graph [20], A* [21] and Dijkstra algorithms [22], but the path planning of a multi-robot team is out of scope in this paper; we will not describe the path planning methods in detail. Third, multiple objects are assumed to be gathered together before object transportation such that

$$\|p^{O_{i+1}} - p^{O_i}\| < r_{i+1} + r_i + \varepsilon \text{ for } \forall i, \quad (1)$$

where $p^{O_i} \in R^2$ and r_i are the position and radius of the i^{th} object O_i , respectively, as shown in Fig.2. The coefficient ε is a marginal constant between objects. The index i is given according to the order of relative distance between objects. For example, object O_{i+1} is the closest object to an object O_i among all objects. Fourth, symmetrical robot formation is assumed to be prepared in advance before object transportation. In this paper, we will not describe an approaching phase so as to concentrate on the transportation process; however, if we need it, various approaching methods of multi-robot (e.g., artificial potential field method [23] or sheep flocking behavior [24]) can be applied to the proposed technique. Fifth, we assume that the sizes and number of objects are known in advance. Finally, all obstacles are convex polygons in which no line segment between two points on the boundary ever goes

outside the polygon, as shown in Fig. 3(a) [25]. In other words, all interior angles of the convex polygon are less than 180° . This is because a small-sized object can be stuck if surrounding obstacles have concave hulls or parabolic shapes, as shown in Fig. 3(b).

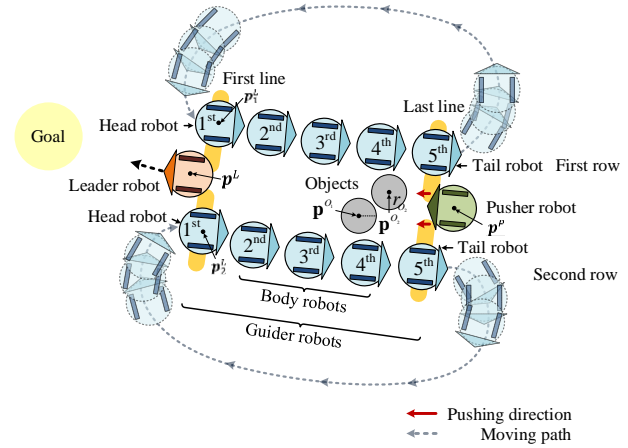


Figure 2. Conceptual illustration of the proposed multi-object transportation. Obstacles are not illustrated in this figure for concentrating on robot formation.

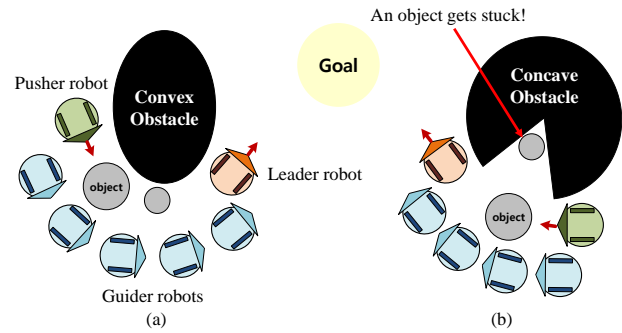


Figure 3. Possible scenarios of object transportation in the environments where convex and concave obstacles exist. (a) Objects are not trapped by convex obstacles during transportation. (b) Small-sized object can be stuck by concave obstacles in a particular case. In this case, robots cannot get into a concave-shaped structure to transport the object because robot's size is larger than the gap of a concave obstacle.

B. Problem Formulation

Object transportation succeeds if all objects are transported to the goal by a multi-robot team. The success of transportation is defined as:

$$\|p_{GOAL} - p^{O_i}\| \leq \delta \text{ for } \forall i \quad (2)$$

where $p_{GOAL} \in R^2$ is the goal point, p^{O_i} is the position of the i^{th} object, and δ is the radius of the goal. The radius δ increases as more objects are used for transportation; multiple objects cannot arrive at a goal within a small boundary at the same time.

III. PRELIMINARIES

A. The Roles of Robots

The proposed object transportation technique is based on a robot formation using cyclic shift motion [18]. A multi-robot team generates and changes its formation, and it consists of three different roles: *guider*, *leader* and

pusher robots. The guider robots prevent the objects from escaping by lining up with two rows, as shown in Fig.3; their role is similar to sidewalk blocks which guide the right direction to pedestrians. Some of the guider robots have other names: *head*, *tail* and *body robot*. The head and tail robots are located at the first and the last lines of each row, respectively, and the body robot indicates the remainder of guider robots. The leader robot leads the robot team to a goal according to a global path planner. Initially, the leader robot can determine a reference point called a virtual robot, which becomes the head robot afterward. The pusher robot is located between tail robots and it pushes the objects from behind to a goal.

B. Virtual Electric Dipole Field Generation for Cyclic Motion

A key role of the proposed multi-robot team is the guider robot. A corridor made by robots is extended by the cyclic motion of guider robots; two tail robots in each row move to the first line of rows, respectively, as shown in Fig.2. Tail robots should approach head robots from a specific direction for lining up two rows because guider robots have nonholonomic characteristics. A virtual electric dipole field (VEDF) has a specific directional approaching vector field, and thus, we adopt this field for the path generation of guider robots [19], [26]. The simple inducement of the electric dipole field $f^e(x, y)$ is described as follows:

$$f^e(x, y) = \begin{bmatrix} \cos^2 \varphi - \alpha \sin^2 \varphi \\ \sin \varphi \cos \varphi + \alpha \sin \varphi \cos \varphi \end{bmatrix}, \quad (3)$$

where $\varphi = \tan^{-1}(y/x)$ and α is a curvature parameter.

C. Robot Controller

A bang-bang controller is used for the robot controller of proposed technique [27]. The desired angular velocity $\omega_c^d(t+1)$ is calculated as follows:

$$\omega_s(t) = \frac{\gamma_t(t) - \gamma_c(t)}{\Delta T} + [2\alpha_{max} |\gamma_t(t) - \gamma_c(t)|]^{\frac{1}{2}} \text{sgn} \left(\frac{\gamma_t(t) - \gamma_c(t)}{\Delta T} - \omega_c(t) \right) \quad (4)$$

$$\omega_c^d(t+1) = \omega_c(t) + \mu \left(\frac{\omega_s(t)}{\Delta T}, \alpha_{max} \right) \Delta T, \quad (5)$$

where the index t denotes the time, $\omega_c(t)$ is current angular velocity, $\text{sgn}(\cdot)$ is the sign operator, ΔT is the sampling time interval, and $\mu(a, b)$ is clamping function.

The desired tangential velocity $v_c^d(t+1)$ is calculated as follows:

$$v_s(t) = v_t(t) - v_c(t) \cos(e_y(t)) + \omega_t(t) e_y(t) + [2\alpha_{max} |e_x(t)|]^{\frac{1}{2}} \text{sgn}(e_x(t)), \quad (6)$$

$$v_c^d(t+1) = v_c(t) + \mu \left(\frac{v_s(t)}{\Delta T}, \alpha_{max} \right) \Delta T, \quad (7)$$

where $e_x(t)$, $e_y(t)$, and $e_\gamma(t)$ are the tangential, lateral and angular path error at time t , respectively.

IV. COOPERATIVE OBJECT TRANSPORTATION IN A STATIC ENVIRONMENT

The method proposed in this paper is an extended object transportation method from the previously proposed

method based on cyclic shift motion [18], [28]. To apply the previously proposed technique to a static environment, three major modifications are required as follows. First, the origin selection method of VEDF should be modified because the back of the head robot can be an obstacle. In the existing technique, the origin of VEDF was the next head robot. If a moving guider robot follows the existing origin selection rule, the guider robot will collide with obstacles, as shown in Fig.1(a). Therefore, the leader robot takes the role of determining the origin of VEDF considering surrounding static obstacles. Second, the state transition method of guider robots should be modified. In the existing proposed technique, the state transition totally depends on the lining-up order of guider robots by the gradient algorithm. However, the lining-up order cannot be calculated due to obstacles in a static environment. Therefore, a new command architecture is necessary for the state transitions of guider robots. Finally, the robot formation can be asymmetric due to obstacles, as shown in Fig.1(c). Thus, a new formation maintenance method should be introduced because the existing proposed technique considers only symmetric cases.

We can solve the above problems by giving more authority to the leader robot as follows. For example, the origin of VEDF is assigned with respect to the position of the leader robot, not the head robot. The guider robots can generate the VEDF using this method whether obstacles exist or not. In addition, the leader robot orders guider robots to change their states via neighboring communications. Finally, symmetrical formation is rearranged by the command of the leader robot after all guider robots pass through the region where obstacles exist.

V. FINITE STATE MACHINES

A. Event Descriptions of FSMs

Finite state machines (FSMs) for object transportation are presented as shown in Fig.4 and Table I. The value s_θ^i is the measured distance of sensor's θ -direction with respect to robot $i \in \{\text{Leader}, \text{Pusher}, \text{Guider}\}$. The degree θ increases counter clockwise with respect to robot's heading. The positions \mathbf{p}^L , \mathbf{p}_1^L , \mathbf{p}_2^L , \mathbf{p}^P are depicted as in Fig.2, and the \mathbf{p}_{self}^G means the position of the current guider robot.

TABLE I. THE EVENTS OF FSMS IN A STATIC ENVIRONMENT

Robot	Event	Descriptions		Commander
		1 st row	2 nd row	
Guider	E_1^G	$s_{\pi/3}^L \geq s_{max}$	$s_{-\pi/3}^L \geq s_{max}$	Leader
	E_2^G	$\ \mathbf{p}_{self}^G - \mathbf{p}^L\ < 2r + s_{max}$		Leader
	E_3^G	$\ \mathbf{p}_{self}^G - \mathbf{p}_1^L\ < s_\epsilon$	$\ \mathbf{p}_{self}^G - \mathbf{p}_2^L\ < s_\epsilon$	Guider
Pusher	E_1^P	$s_{\pi/2}^P \geq s_{max}$ or $s_{-\pi/2}^P \geq s_{max}$ or $\ \mathbf{p}_i^G - \mathbf{p}^P\ > s_{max}$ for $\forall i$		Pusher
	E_2^P	$s_{\pi/2}^P < s_{max}$ and $s_{-\pi/2}^P < s_{max}$		Pusher
Leader	E_1^L	$s_{\pi/2}^L < s_{max}$ and $s_{-\pi/2}^L < s_{max}$		Leader
	E_2^L	$s_{\pi/2}^L \geq s_{max}$ or $s_{-\pi/2}^L \geq s_{max}$		Leader

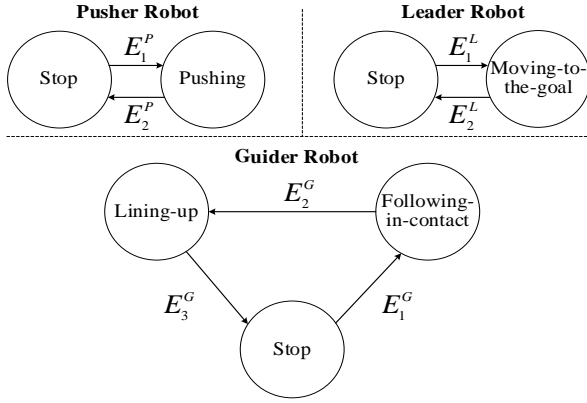


Figure 4. The finite state machines of guider, pusher, and leader robots

B. The States of Guider Robot

For guider robots, the following-in-contact state is presented in Algorithm 1. Guider robots move along the robot formation or surrounding obstacles when the state of a guider robot is the following-in-contact. The turning direction of guider robots depends on where they are lined up. For example, the guider robot moves forward and turns counter clockwise if a guider robot is lined up in the first row. In the lining-up state, the guider robot which belongs to the first and second row generates two VEDFs with respect to the right (\mathbf{p}_1^L) and left reference points (\mathbf{p}_2^L) of the leader robot, respectively. These reference points are as follows:

$$\mathbf{p}_1^L = \mathbf{p}^L + \begin{bmatrix} (2r + \varepsilon) \cos(\gamma^L - \frac{\pi}{2}) \\ (2r + \varepsilon) \sin(\gamma^L - \frac{\pi}{2}) \\ \varphi \end{bmatrix},$$

$$\mathbf{p}_2^L = \mathbf{p}^L + \begin{bmatrix} (2r + \varepsilon) \cos(\gamma^L + \frac{\pi}{2}) \\ (2r + \varepsilon) \sin(\gamma^L + \frac{\pi}{2}) \\ \varphi \end{bmatrix}, \quad (8)$$

where \mathbf{p}^L is the position of the leader robot, and γ^L is the target heading angle of leader robot. In (8), the third element φ of matrix indicates the rotational angle of VEDF. The target heading angle and rotational angle of VEDF are determined by the global path planner of the leader robot. The lining-up state algorithm is described in Algorithm 2.

Algorithm 1. following-in-contact (for guider robot)

Input: the sensor information of guider robot, s_θ^G
Output: action of the guider robot

```

while the state of guider robot is in following-in-contact do
    if  $\forall s_\theta^G \geq s_{\max}$  then
        | move forward and {counterclockwise1st, clockwise2nd}
    else if  $s_{\pi/2}^G < s_{\text{desired}}$  or  $s_{-\pi/2}^G < s_{\text{desired}}$ 
        | move forward and {clockwise1st, counterclockwise2nd}
    else if  $s_{\text{desired}} < s_{\pi/2}^G \leq s_{\max}$  or
        |  $s_{\text{desired}} < s_{-\pi/2}^G \leq s_{\max}$ 
        | move forward and
        | {counterclockwise1st, clockwise2nd}
    else
        | move straight forward
    end
end
end
    
```

Algorithm 2. lining-up (for guider robot)

Input: the position of leader robot, \mathbf{p}^L
 the desired origins of VEDF with respect to the relative row (1st and 2nd rows), $\mathbf{p}_1^L, \mathbf{p}_2^L$

Output: the desired tangential velocity of the guider robot, (v^d, ω^d)

```

while the state of guider robot is in lining-up do
    generate virtual electric dipole field  $f^e(x, y)$  using (3) according to
    the local coordinate of  $\mathbf{p}_1^L$  or  $\mathbf{p}_2^L$  with respect to the relative row.
    approach the desired position using  $(v^d, \omega^d)$  by (5) and (7),
    respectively.
end
    
```

The control decision of guider robots is based only on their own sensor value s_θ^G and the position of the leader robot \mathbf{p}^L , as described in Algorithm 1 and 2. In the lining-up state, the position of the leader robot can be estimated using the guider robot's own sensor, and thus, the guider robots are controlled by decentralized method. In other words, the proposed method is robust to fault scenarios such as unexpected faults or communication failures. For example, if some guider robots have operational problems, the leader robot excludes the problematic robots from the multi-robot team, then can give an order to the next guider robot. However, if there is a problem with the leader or pusher robot, it cannot be solved because of their own particular roles such as pushing and path planning.

C. The States of Pusher Robot

For the pusher robot, the stop state is identical to the previously proposed technique [18], and thus, we will explain briefly. The pusher robot stops pushing objects until there exist guider robots or obstacles on both sides. In the pushing state, the pusher robot does not transmit commands to other robots, unlike the previously proposed technique. The pusher robot takes a pushing action only using the relative distance from guider robots, which is a decentralized control. The algorithm for the pushing state is described in Algorithm 3.

Algorithm 3. pushing (for pusher robot)

Input: the sensor information of pusher robot, s_θ^P
Output: action of the pusher robot

```

while the state of pusher robot is in pushing do
    if  $\forall s_{\pi/2}^G \geq s_{\max}$  then
        | move forward and counterclockwise
    else if  $s_{-\pi/2}^G \geq s_{\max}$ 
        | move forward and clockwise
    else
        | move straight forward
    end
end
end
    
```

D. The States of Leader Robot

For the leader robot, the moving-to-the-goal state is identical to that of the previously proposed technique [18]. The global path planner has a feasible path-planning trajectory considering multiple obstacles, and it can be generated by diverse path planning algorithms such as A* [20] or visibility graph [21]. In the stop state, the leader robot orders guider robots to change their states according to the sensor information of the leader and the states of the guider robot. Algorithm 4 shows the stop state in a static environment. If the states of all guider robots are stop state, the leader robot orders the tail robot to change its state to

the following-in-contact. If the distance between the guider robot and the desired origin of VEDF is less than the sensing range, the leader robot orders the $(-1)^{\text{th}}$ moving guider robot to change to the lining-up state. The orders of the leader robot are transmitted via wireless communications between neighboring guider robots.

Algorithm 4. stop (for leader robot)

Input: the state of j^{th} guider robot in i^{th} row, $A_{(i,j)}^G$
 the position of guider robot which belongs to following-in-contact state, p_{-1}^G
 the sensor information of leader robot, s_{θ}^L
Output: action of the leader robot

```

while the state of leader robot is in stop do
     $v^L \leftarrow 0$ 
    if  $\forall A_{(i,j)}^G = \text{stop}$  then
        if  $s_{\pi/3}^L \geq s_{\max}$  then
             $A_{(1,\text{tail})}^G \leftarrow \text{following-in-contact}$ 
        end
        if  $s_{-\pi/3}^L \geq s_{\max}$  then
             $A_{(2,\text{tail})}^G \leftarrow \text{following-in-contact}$ 
        end
    end
    if  $\|p_{-1}^G - p_1^L\| < 2r + s_{\max}$  then
         $A_{(1,-1)}^G \leftarrow \text{lining-up}$ 
    end
    if  $\|p_{-1}^G - p_2^L\| < 2r + s_{\max}$  then
         $A_{(2,-1)}^G \leftarrow \text{lining-up}$ 
    end
end
    
```

VI. SIMULATIONS

A. Simulation Environment

In our simulations, a multi-robot team consists of 14 guider robots, a leader robot, and a pusher robot. All robots have identical radii, which is 10 cm. Our purpose is to transport two objects of which radii are 14 cm and 12 cm, respectively. The environmental size is 700×200 cm. We used one or more rectangular obstacles, which are convex-shaped obstacles. The size of a rectangular obstacle is 100×65 cm. Capital characters mean robot name in descriptions: guider (G), leader (L) and pusher (P) robots.

B. An Obstacle Case

We simulated the proposed technique in an environment where a single rectangular-shaped obstacle exists, as shown in Fig.5. The leader robot could not detect anything on its left side; an obstacle was located on its right side, as shown in Fig.5 at 0 second. Therefore, the leader robot ordered the tail robot (G1) located in the second row to change its state from the stop to following-in-contact. Then, the G1 robot began to follow the boundary of the second row, as shown in Fig.5 at 1 second. When the G1 robot approached the origin of VEDF, its state was changed by the leader robot’s order from the following-in-contact to lining-up state. Likewise, the G2, G3, and G4 robots showed similar actions. At 26 second, two tail robots (G5 and G8) in the first and second rows began to move together because the leader robot detected that there were no robots or obstacles on both sides. This means that there is no obstacle on both sides of the leader robot. The guider robots avoided the obstacle in the following-in-contact state while they moved. The guider robots showed the similar actions by the lining-up state after the robots passed

the obstacles. The proposed multi-robot team succeeded in two-object transportation, and the total travel time was 138 seconds.

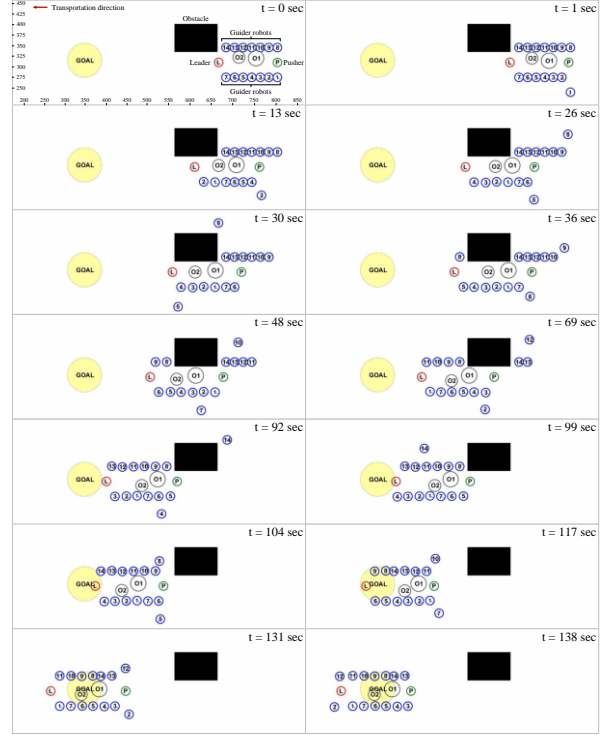


Figure 5. Simulation result in a static environment where a rectangular obstacle exists.

C. Two Obstacles Case

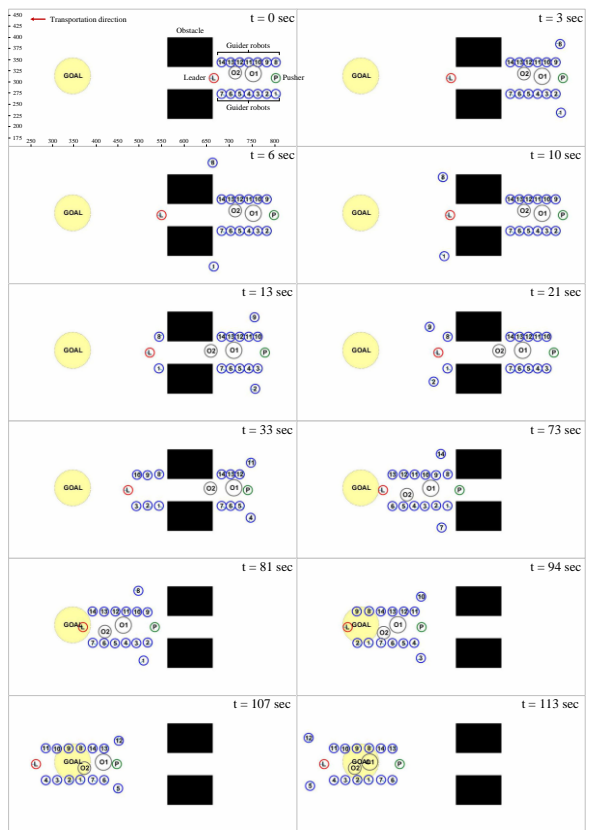


Figure 6. Simulation result in a static environment where two rectangular obstacles exist.

We also simulated the proposed technique in an environment where two obstacles exist, as shown in Fig.6. The objects were transported by passing through the gap between the rectangular obstacles. When the pusher robot was located between obstacles, it pushed objects along the obstacles, as shown in Fig. 6 at 73 seconds. In this case, two obstacles took the role of guider robots. The obstacles were successfully transported in 113 seconds. This travel time was shorter than the one-obstacle case because two obstacles helped to shorten the travel distance that the guider robots should move.

D. A Comparative Experiment

To compare with the existing technique, we performed caging object transportation in a static environment [15], as shown in Fig.7. In the caging technique, robots approach and enclose the target objects with a circular formation. And then, robots transport objects to a goal with orbital motion after the enclosing formation was generated. Initially, robots succeeded in approaching objects from 1 to 3 seconds. However, the enclosing formation of the robots was broken due to obstacles' path disturbance after 7 seconds. Finally, the object (O2) escaped from the robot formation, and thus, object transportation failed.

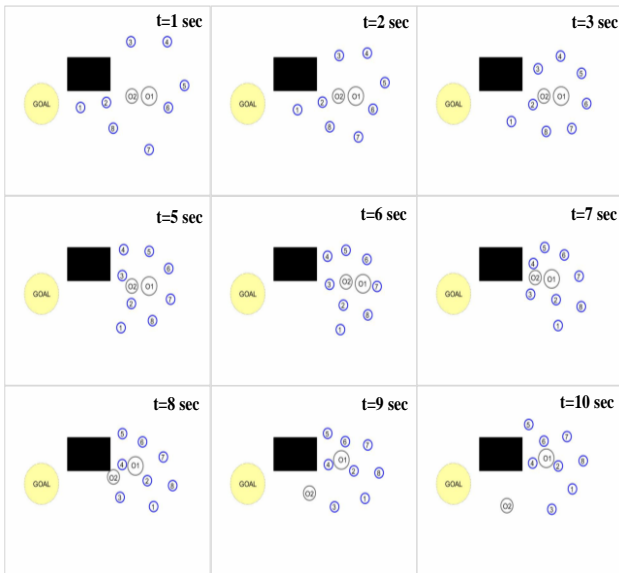


Figure 7. A comparative simulation result (caging technique) [15]. Eight robots approached two objects and enclosed them with orbital motion after 1 second. However, robots could not build an enclosing formation due to a rectangular obstacle. The object (O2) began to escape from the enclosing robot formation after 8 seconds. Finally, robots' formation was broken, and object transportation failed.

VII. PRACTICAL EXPERIMENT

A. Experimental Environment

We used a pusher, a leader, and 6 guider robots for practical experiments. E-puck robots were used as pusher and guider robots, and the elisa-3 robot was used as a leader robot. The multiple objects are a paper cup and a ping-pong ball. The sensing range of e-puck and elisa-3 robots was less than 6 cm. The size of the rectangular-shaped box was 15×7 cm. ID tags were attached to the

robots for position tracking. The visual tracking system can estimate robots' position in real-time using an overhead camera. This position information acquired from the visual tracking system was used only for recording trajectories of robots, objects, and an obstacle; each robot was not provided with the positions of other robots via the visual tracking system.

B. Experimental Result

We also conducted a practical experiment in a static environment. The shape of the obstacle is a rectangle, as shown in Fig.8 at 0 second. At first, a leader robot began to move-to-the-goal by event E_1^L because there were two guider robots on both sides. When the leader robot arrived at the position where there were no guider robots on both sides, it stopped and ordered tail robots to move according to the event E_1^G , as shown in Fig.8 at 8 seconds. Then, the tail robots approached the head robots by the following-in-contact and lining-up states. To approach the head robots, the guider robots followed the row of guider robots at 30 seconds. If the guider robots were close to the leader robot, they generated and followed the VEDF with respect to the relative position of the leader robot. At the same time, a pusher robot pushed the objects, as shown in Fig.8 at 30 seconds. The leader robot ordered the guider robot to locate in the second row because there was an obstacle in the first row only, after 48 seconds. Therefore, the guider robots in the second row (G4, G5, and G6) moved alone while the leader robot passed the obstacle. Two guider robots in both rows moved together after the guider robots passed through the region located in the obstacle, as shown in Fig. 8 at 163 seconds. The remaining processes were analogous to the previous steps. The total travel time was 363 seconds, and the trajectories of robots are illustrated in Fig.9.

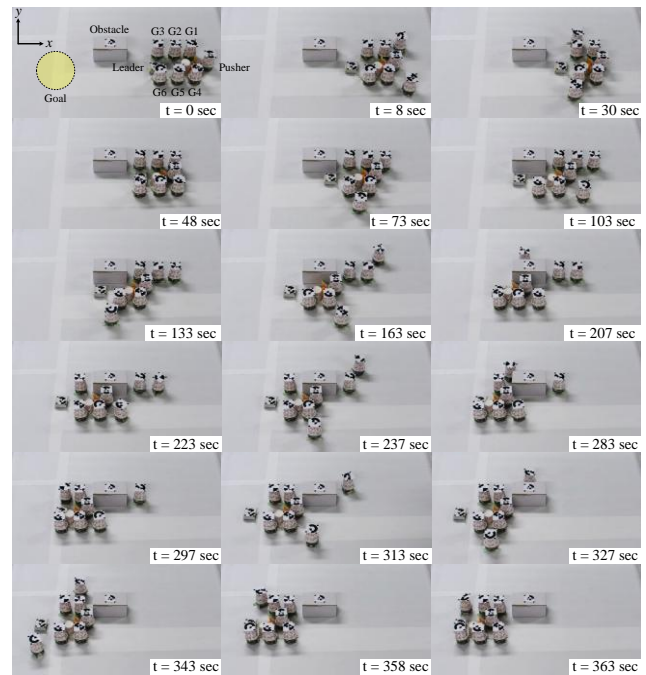


Figure 8. Object transportation in a static environment. A rectangular-shaped box prevents the objects from escaping.

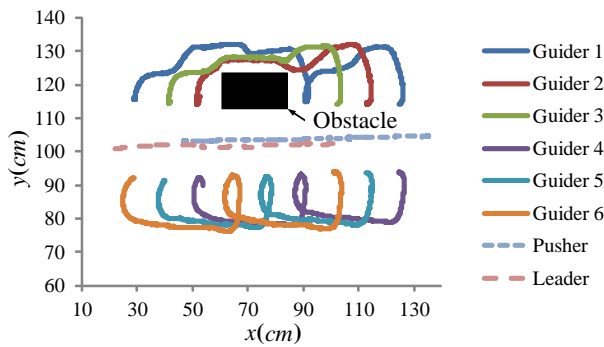


Figure 9. The trajectories of the robots during the transportation

VIII. CONCLUSION

In this paper, we propose a multi-object transportation technique exploiting surrounding obstacles. Robots could transport multiple objects easily, with the help of surrounding obstacles. A leader robot designed a guided path, considering surrounding obstacles. A pusher and guider robots take actions according to their FSMs with decentralized methods. In this case, obstacles are not a hindrance anymore for object transportation. The proposed technique can be utilized in various fields where there exist many static objects, such as foraging, space exploration, and logistics.

CONFLICT OF INTEREST

The authors declare no conflict of interest.

REFERENCES

- [1] C. Rizzo, A. Lagrana, and D. Serrano, "GEOMOVE: Detached AGVs for cooperative transportation of large and heavy loads in the aeronautic industry," 2020.
- [2] P. S. Schenker, T. L. Huntsberger, P. Pirjanian, E. T. Baumgartner, and E. Tunstel, "Planetary rover developments supporting mars exploration, sample return and future human-robotic colonization," *Auton. Robots*, vol. 14, no. 2-3, 2003.
- [3] J. Hu, P. Bhowmick, I. Jang, F. Arvin, and A. Lanzon, "A decentralized cluster formation containment framework for multirobot systems," *IEEE Trans. Robot.*, 2021.
- [4] O. Zedadra, H. Seridi, N. Jouandea, and G. Fortino, "A cooperative switching algorithm for multi-agent foraging," *Eng. Appl. Artif. Intell.*, vol. 50, 2016.
- [5] O. Feinerman, I. Pinkoviezky, A. Gelblum, E. Fonio, and N. S. Gov, "The physics of cooperative transport in groups of ants," *Nature Physics*, vol. 14, no. 7, 2018.
- [6] A. Rajasekhar, N. Lynn, S. Das, and P. N. Suganthan, "Computing with the collective intelligence of honey bees – A survey," *Swarm and Evolutionary Computation*, vol. 32, 2017.
- [7] J. Hu, P. Bhowmick, and A. Lanzon, "Group coordinated control of networked mobile robots with applications to object transportation," *IEEE Trans. Veh. Technol.*, 2021.
- [8] R. Groß, E. Tuci, M. Dorigo, M. Bonani, and F. Mondada, "Object transport by modular robots that self-assemble," in *Proc. IEEE International Conference on Robotics and Automation*, 2006, vol. 2006.
- [9] R. Groß, F. Mondada, and M. Dorigo, "Transport of an object by six pre-attached robots interacting via physical links," in *Proc. IEEE International Conference on Robotics and Automation*, 2006, vol. 2006.
- [10] Z. Liu, H. Kamogawa, and J. Ota, "Fast grasping of unknown objects through automatic determination of the required number of mobile robots," *Adv. Robot.*, vol. 27, no. 6, 2013.
- [11] M. J. Mataric, M. Nilsson, and K. T. Simsarian, "Cooperative multi-robot box-pushing," in *IEEE International Conference on Intelligent Robots and Systems*, 1995, vol. 3.
- [12] T. Meriçli, M. Veloso, and H. L. Akin, "Push-manipulation of complex passive mobile objects using experimentally acquired motion models," *Auton. Robots*, vol. 38, no. 3, 2015.
- [13] M. De Berg and D. H. P. Gerrits, "Computing push plans for disk-shaped robots," *Int. J. Comput. Geom. Appl.*, vol. 23, no. 1, 2013.
- [14] B. P. Gerkey and M. J. Mataric, "Pusher-watcher: An approach to fault-tolerant tightly-coupled robot coordination," in *Proc. IEEE International Conference on Robotics and Automation*, 2002, vol. 1.
- [15] G. A. S. Pereira, M. F. M. Campos, and V. Kumar, "Decentralized algorithms for multi-robot manipulation via caging," *International Journal of Robotics Research*, 2004, vol. 23, no. 7-8.
- [16] A. Rodriguez, M. T. Mason, and S. Ferry, "From caging to grasping," *Int. J. Rob. Res.*, vol. 31, no. 7, 2012.
- [17] J. Fink, M. Ani Hsieh, and V. Kumar, "Multi-robot manipulation via caging in environments with obstacles," 2008.
- [18] G. Eoh, J. D. Jeon, J. H. Oh, and B. H. Lee, "Cooperative object transportation using parallel line formation with a circular shift," *Robotica*, vol. 35, no. 6, 2017.
- [19] G. Eoh, J. Do Jeon, and B. H. Lee, "Cooperative object transportation using virtual electric dipole field," *Int. J. Mech. Eng. Robot. Res.*, vol. 5, no. 1, 2016.
- [20] H. P. Huang and S. Y. Chung, "Dynamic visibility graph for path planning," in *2004 IEEE/RSJ International Conference on Intelligent Robots and Systems (IROS)*, 2004, vol. 3.
- [21] S. M. Persson and I. Sharf, "Sampling-based A* algorithm for robot path-planning," *Int. J. Rob. Res.*, vol. 33, no. 13, 2014.
- [22] G. Z. Tan, H. He, and A. Sloman, "Global optimal path planning for mobile robot based on improved Dijkstra algorithm and ant system algorithm," *J. Cent. South Univ. Technol. (English Ed.)*, vol. 13, no. 1, 2006.
- [23] J. Ren, K. A. McIsaac, R. V. Patel, and T. M. Peters, "A potential field model using generalized sigmoid functions," *IEEE Trans. Syst. Man, Cybern. Part B Cybern.*, vol. 37, no. 2, 2007.
- [24] J. Hu, A. E. Turgut, T. Krajnčič, B. Lennox, and F. Arvin, "Occlusion-based coordination protocol design for autonomous robotic herding tasks," *IEEE Trans. Cogn. Dev. Syst.*, 2020.
- [25] M. Dimakos and A. S. Fokas, "The poisson and the biharmonic equations in the interior of a convex polygon," *Stud. Appl. Math.*, vol. 134, no. 4, 2015.
- [26] D. K. Cheng, "Field and wave electromagnetics," *IEEE Antennas and Propagation Society Newsletter*, vol. 28, no. 2, 1986.
- [27] K. C. Koh and H. S. Cho, "Smooth path tracking algorithm for wheeled mobile robots with dynamic constraints," *J. Intell. Robot. Syst. Theory Appl.*, vol. 24, no. 4, 1999.
- [28] G. Eoh, "An Approach to Cooperative Robot Behavior for Object Transportation," Ph.D. Dissertation, Dept. of Electrical Engineering and Computer Science, Seoul National University, 2016.

Copyright © 2022 by the authors. This is an open access article distributed under the Creative Commons Attribution License (CC BY-NC-ND 4.0), which permits use, distribution and reproduction in any medium, provided that the article is properly cited, the use is non-commercial and no modifications or adaptations are made.



Gyuho Eoh received B.S., M.S., and Ph.D degrees in electrical engineering and computer science from Seoul National University, Korea, in 2009, 2011, and 2016, respectively. From March 2016 to December 2020, he was a senior engineer in LG Electronics CTO division (advanced robotics lab.), where his research focused on fusion SLAM. He is now a research professor at Chungbuk National University, and his current research interests are multi-robot cooperation, deep reinforcement learning, SLAM, and decision-making in autonomous vehicles.